

Catalytic Cracking of Used Palm Oil and Palm Oil Fatty Acids Mixture for the Production of Liquid Fuel: Kinetic Modeling

Yean-Sang Ooi, Ridzuan Zakaria, Abdul Rahman Mohamed, and Subhash Bhatia*

School of Chemical Engineering, Universiti Sains Malaysia, Engineering Campus, 14300 Nibong Tebal, SPS, Penang, Malaysia

Received February 23, 2004. Revised Manuscript Received June 24, 2004

Catalytic cracking of palm-oil-based fatty acids mixtures (FAM) and used palm oil (UPO) was performed over composite catalysts (HZSM-5 and MCM-41/ZSM-5). The reaction was studied in the temperature range of 673–723 K and a weight hourly space velocity of WHSV = 2.5–4.5 h⁻¹ in a fixed-bed microreactor. A lumped parameter model was proposed to represent the catalytic cracking kinetics of FAM and UPO. The sequential strategy was used to estimate the lumped kinetic constants for three-, four- and six-lump models. The role of the catalyst in the product distribution was determined from the kinetic model that was proposed. The conversion and yield of different products predicted by the six-lump model showed good agreement with the experimental data.

1. Introduction

Over the past few decades, the issue of developing alternative fuel has been an area of research, especially bio-fuel produced from the catalytic cracking of vegetable oil.^{1–3} Bio-fuel from vegetable oil provides not only a sustainable energy source but also environmental benefits (less toxic gas emission and greenhouse effect). Therefore, the large-scale production of biofuel to meet the increasing demand in the transportation sector is of greater interest. To provide useful information for the design of catalytic reactor, a suitable kinetic model must be developed.

Because of the complexity of the reactions and the large number of components involved in the cracking process, it is difficult to describe the kinetics of bio-fuel at the molecular level. Hence, lumping the components with a similar nature into a few categories of pseudo-components is necessary for the development of a suitable kinetic model.⁴ The three-lump model was proposed for gas oil cracking by Weekman,⁵ by grouping the components as unconverted gas oil, gasoline, and gas plus coke. Many efforts were reported to describe the process by separating the products into more lumps.^{4,6–8} The activity of the catalyst decreases with

time in the cracking reaction. To represent the kinetics of gas oil cracking precisely, the deactivation function was incorporated in the model. The catalyst activity model was generally assumed to follow the exponential law as a function of the time-on-stream.^{4,6,7,9}

In the present study, used palm oil (UPO) was used as feedstock, to make the process more economically viable. Another feedstock, fatty acids mixture (FAM), was also used. Both feeds were cracked over a HZSM-5 catalyst to study their product distribution. To investigate the influence of the pore size of the catalyst in the product distributions, a mesoporous composite catalyst (MCM-41) and a microporous composite catalyst (ZSM-5) were synthesized and used for the cracking in the present study. The reaction parameters for the catalytic cracking of UPO and FAM were evaluated based on the proposed kinetic model.

2. Experimental Section

2.1. Catalyst Preparation. *2.1.1. HZSM-5.* NH₄-ZSM-5 with a Si/Al ratio of 40 was obtained from Zeolyst International, USA. The NH₄-ZSM-5 sample was calcined in a muffle furnace for 6 h at 873 K to obtain HZSM-5.

2.1.2. Composite MCM-41/ZSM-5. The composite catalyst was prepared by coating ZSM-5 with a layer of mesoporous material, using cetyltrimethylammonium chloride (C₁₆TMACl) as a template, following the procedure reported by Kloetstra et al.¹⁰ with some modifications. The purely siliceous MCM-

* Author to whom correspondence should be addressed. Telephone: 604 5937788. Fax: 604 5941013. E-mail: chbhatia@eng.usm.my.

(1) Katikaneni, S. P. R.; Adjaye, J. D.; Bakhshi, N. N. *Can. J. Chem. Eng.* **1995**, *73*, 484–497.

(2) Adjaye, J. D.; Katikaneni, S. P. R.; Bakhshi, N. N. *Fuel Process. Technol.* **1996**, *48*, 115–143.

(3) Twaiq, F.; Zabidi, N. A. M.; Bhatia, S. *Ind. Eng. Chem. Res.* **1999**, *38*, 3230–3238.

(4) Ancheyta-Juarez, J.; Lopez-Isunza, F.; Aguilar-Rodriguez, E.; Moreno-Mayorga, J. C. *Ind. Eng. Chem. Res.* **1997**, *36*, 5170–5174.

(5) Weekman, V. M. *Ind. Eng. Chem. Prod. Res. Dev.* **1968**, *7*, 90–95.

(6) Abul-Hamayel, M. A. *Fuel* **2003**, *82*, 1113–1118.

(7) Ancheyta-Juarez, J.; Lopez-Isunza, F.; Aguilar-Rodriguez, E. *Appl. Catal., A* **1999**, *177*, 227–235.

(8) Jacob, S. M.; Gross, B.; Voltz, S. E.; Weekman, V. M. *AIChE J.* **1976**, *22*, 701–713.

(9) van Landeghem, F.; Nevicato, D.; Pitault, I.; Forissier, M.; Turlier, P.; Derouin, C.; Bernard, J. R. *Appl. Catal., A* **1996**, *138*, 381–405.

(10) Kloetstra, K. R.; Zandbergen, H. W.; Jansen, J. C.; Bekkum, H. V. *Microporous Mater.* **1996**, *6*, 287–293.

41 gel was prepared using the method reported by Lindlar et al.¹¹ A quantity (15.4 g) of hexadecyltrimethylammonium chloride solution (25%, Fluka) and 0.08 g of ammonia solution (25%, Merck) were mixed in beaker I, and 12.0 g of sodium silicate solution (27% SiO₂, 10% NaOH, Riedel-deHaen) and 0.36 g of Cab-o-Sil M5 (Fluka) were mixed with 14 mL of deionized water in beaker II. The contents of beaker II were slowly added to beaker I, with vigorous stirring at room temperature. The mixture was stirred for 15 min at room temperature before the powder zeolite ZSM-5 was added. The resultant composite gel was heated at 373 K for 24 h without stirring. The mixture was then cooled to room temperature and the pH was adjusted to ~11, via a dropwise addition of acetic acid under vigorous stirring. The reaction mixture was heated to 373 K for 24 h, and this procedure for pH adjustment and heating was repeated twice. The product obtained was filtered, washed with deionized water, and dried at room temperature overnight before being calcined at 823 K for 6 h. The composite of pure siliceous MCM-41 with ZSM-5 was coded as CMZX, where C refers to composite, M refers to MCM-41, Z refers to ZSM-5, and X represents the mesophase weight percent (20 and 40 wt %) in the composite synthesis gel.

2.2. Catalyst Characterization. The XRD patterns of the catalysts were obtained using a Philips diffractometer with Cu K α radiation at $2\theta = 1.5^\circ$ – 90° with a step of $0.04^\circ/10$ s, to determine the structure and composition of crystalline material. The nitrogen sorption characterization of the samples was conducted using Autosorb I (a Quantachrome automated gas sorption system). The Brunauer–Emmett–Teller (BET) surface area and pore volume of the catalysts were measured after the samples were degassed for 5 h under vacuum at 573 K. The acidity of the catalyst was measured using the temperature-programmed desorption (TPD) of ammonia. The TPD was performed using Chembet 3000 (Quantachrome) that was equipped with TPRWin (version 1) software to calculate the acidity. The external shape and morphology of the catalyst was examined using scanning electron microscopy (Leica Cambridge model S-360). Transmission electron microscopy (TEM) images were obtained using a Philips model CM12 transmission electron microscope that was operated at an acceleration voltage of 80 kV.

2.3. Kinetic Studies. The catalyst activity was measured at reaction temperatures of 673, 698, and 723 K at atmospheric pressure in a fixed-bed microreactor rig. The FAM/UPO feed rate (weight hourly space velocity, WHSV) was varied over a range of 2.5–4.5 h⁻¹. Each feedstock was tested over HZSM-5 and composite MCM-41/ZSM-5, to study the effect of the addition of MCM-41. The fatty acids compositions of the feedstocks are given in Table 1; these data were obtained from the analysis of feedstock samples using gas chromatography–mass spectroscopy (GC–MS). The deactivation of the catalysts was studied by changing the catalyst/oil ratio in the range of 0.1–0.167. Twenty seven experiments based on the design of experiment were conducted for each feedstock over each catalyst. In each run, 1.0 g of fresh catalyst was loaded over 0.2 g of quartz wool supported with a stainless-steel mesh in the microreactor (185 mm \times 10 mm inner diameter (ID)) placed in the vertical tube furnace (Model No. MTF 10/25/130, Carbolite). The reactor temperature was monitored by a thermocouple that was positioned in the center of the catalyst bed. Nitrogen gas was passed through the reactor for 1 h before the FAM/UPO was fed using a syringe pump (Model No. E-74900-05, Cole–Parmer). The liquid product was collected in a glass liquid sampler, while the gaseous products were collected in a gas-sampling bulb, after the steady state was attained in the reactor. The residue oil was separated from the liquid product by distillation in a microdistillation unit

Table 1. Fatty Acid Composition of the Feedstock

fatty acid	Composition (wt %)	
	fatty acids mixture (FAM)	used palm oil (UPO)
lauric acid (C12:0)	3.23	1.03
myristic acid (C14:0)	1.59	2.34
palmitic acid (C16:0)	6.11	22.47
palmitoleic acid (C16:1)		7.56
heptadecanoic acid (C17:0)		0.48
stearic acid (C18:0)	8.25	12.51
oleic acid (C18:1)	68.64	27.64
linoleic acid (C18:2)	7.00	14.58
linolenic acid (C18:3)		1.55
arachidic acid (C20:0)	1.80	0.64
eicosenoic acid (C20:1)	1.05	
eicosadienoic acid (C20:2)		0.29
arachidonic acid (C20:4)		0.37
behenic acid (C22:0)	0.59	
lignoceric acid (C24:0)	1.21	
others	0.53	8.54

(Buchi B850, GKR) at 473 K for 30 min under vacuum (100 Pa) with the pitch serving as residual oil. The spent catalyst was washed with acetone prior to the coke analysis. The amount of coke was determined by the difference before and after calcination in a muffle furnace.

The gaseous products were analyzed over a gas chromatograph (Model 5890 series II, Hewlett-Packard) using a Hewlett-Packard HP Plot Q capillary column (divinyl benzene/styrene porous polymer, 30 m long \times 0.53 mm ID \times 40 μ m film thickness) equipped with a thermal conductivity detector (TCD) and using nitrogen as a carrier gas. The organic liquid product (OLP) was analyzed using a capillary glass column (Petrocol DH 50.2, film thickness of 0.5 μ m, 50 m long \times 0.2 mm ID), with a flame ionization detector. The composition of OLP was defined, according to the boiling range of petroleum products, as being comprised of three fractions, i.e., a gasoline fraction (333–393 K), a kerosene fraction (393–453 K), and a diesel fraction (453–473 K).

3. Deactivation Model

The catalysts are subjected to a loss of activity with increasing time-on-stream, because of coking during the cracking reaction. Although the presence of coke was responsible for the deactivation of the catalyst, the use of coke on the catalyst as a measure of catalyst activity was reported to be difficult.¹² Hence, the deactivation model was developed assuming that catalyst activity (φ) is dependent on the time on stream (t) which is a nonselective model. The catalyst activity φ is defined as the ratio of the rate of reaction at time t to the rate of reaction over a fresh catalyst ($t = 0$). The rate of deactivation is given by eq 2.

$$\varphi(t) = \frac{\text{rate of reaction at time } t}{\text{rate of reaction at time } t = 0} \quad (1)$$

$$\frac{d\varphi}{dt} = -k_d \varphi^{n_d} \quad (2)$$

Here, k_d is the deactivation rate constant and n_d is the order of catalyst deactivation.

The rates of FAM and UPO cracking at different time-on-stream values were obtained by changing the total weight of oil injected into the reactor at selected feed rates, which resulted in a change in the total time of the experiment. The values of n_d and k_d were estimated

(11) Lindlar, B.; Kogelbauer, A.; Prins, R. *Microporous Mesoporous Mater.* **2000**, *38*, 167–176.

(12) Wojciechowski, B. W.; Corma, A. *Catalytic Cracking: Catalysts, Chemistry and Kinetics*; Marcel Dekker: New York, 1986.

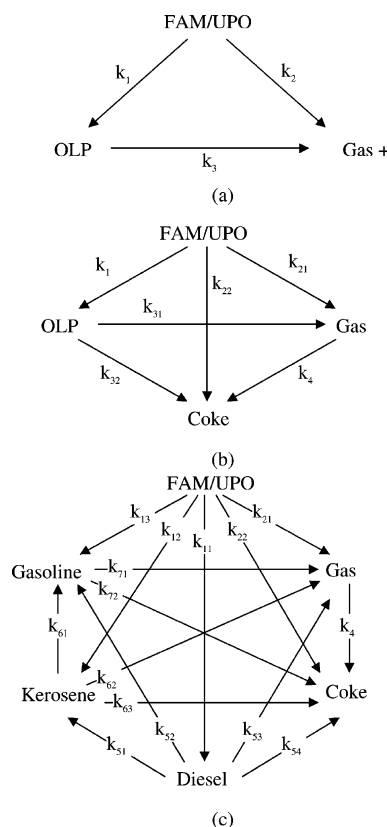


Figure 1. Kinetic scheme for (a) the three-lump model, (b) the four-lump model, and (c) the six-lump model.

Table 2. Deactivation Rate Parameter and Order for Different Feedstock and Catalysts

catalyst	673 K		698 K		723 K	
	k_d	n_d	k_d	n_d	k_d	n_d
FAM Feed						
ZSM-5	0.2681	2	0.3118	1.5	0.2837	1
CMZ20	0.4846	1.3	0.4999	1.5	0.5259	1.5
UPO Feed						
ZSM-5	0.3513	2	0.3883	2	0.3855	2
CMZ40	0.2571	1	0.3834	2	0.4237	2

using nonlinear regression analysis method, based on Levenberg–Marquard’s algorithm. Table 2 presents the values of n_d and k_d obtained in the present study. The integral form of eq 2 gave the value of φ , as shown in eq 3. The φ value was incorporated in the kinetic model, to account for the deactivation of the catalyst.

$$\varphi = [(n_d - 1)k_d t + 1]^{1/(1-n_d)} \quad (3)$$

The value of k_d increased as the reaction temperature increased, whereas the reaction order n_d also varied with the type of feedstock and catalyst used. In FAM cracking, the order of deactivation over the composite catalyst was almost constant at moderate rates. The ZSM-5 deactivation order decreased as the temperature increased. Both catalysts gave the same value of deactivation order in UPO cracking, except at a reaction temperature of 673 K. This was probably due to the presence of 40 wt % of mesoporous MCM-41, which accelerated the rate of coking at low temperature.

4. Kinetic Models

The lumping techniques were used in the present study to estimate the kinetic parameters in the cracking

of FAM and UPO, respectively. Models with a large number of lumps for the evaluation of catalyst are not applicable, because of the limited data available;¹³ therefore, the sequential method was used.⁴ The sequential strategy uses a three-lump model, a four-lump model, and ends with a six-lump model, and this methodology is shown in Figure 1. Using this approach, instead of simultaneous regression of the rate equation involved, the proposed strategy can decrease the number of estimated parameters.

The experimental data (unconverted feedstock and yield of products) were fitted by a suitable polynomial at a catalyst/oil ratio of 0.125 and variation of the residence time ($\tau = 1/\text{WHSV}$). Figure 2 shows the polynomial fitting curves for the cracking of UPO and FAM. The rate of reaction data based on feedstock conversion and products formation for the cracking reaction were determined using a differential method. The conversion and yield of products (organic liquid product (OLP) containing a gasoline fraction, a kerosene fraction, a diesel fraction, gas, and coke) are defined as follows:

$$\text{conversion (wt\%)} = \frac{\text{FAM/UPO feed (wt)} - \text{unconverted feed (wt)}}{\text{FAM/UPO feed (wt)}} \times 100\% \quad (4)$$

$$\text{yield (wt\%)} = \frac{\text{product (wt)}}{\text{FAM/UPO feed (wt)}} \times 100\% \quad (5)$$

The three-lump model, which was comprised of unconverted feedstock, OLP, and gas and coke (Figure 1a) was solved. The weight fraction yields were used, for the convenience of regression analysis. The cracking rate of the FAM/UPO is represented by eq 6:

$$\frac{dC_p}{d\tau} = -k_0 C_p^n \varphi \quad (6)$$

where C_p is the weight percentage of unconverted feedstock and

$$k_0 = k_1 + k_2 \quad (7)$$

The reaction order n was assumed to be the same for all of the reactions. The rate of formation of OLP is given by eq 8, whereas the rate of formation of gas and coke is given by eq 9.

$$\frac{dC_{\text{OLP}}}{d\tau} = (k_1 C_p - k_3 C_{\text{OLP}}) \varphi \quad (8)$$

$$\frac{dC_{\text{gas+coke}}}{d\tau} = (k_2 C_p + k_3 C_{\text{OLP}}) \varphi \quad (9)$$

The rate constants (k_1 , k_2 , and k_3) were determined by nonlinear regression analysis, using the least-squares method. The sum of squares of the errors was minimized using an iterative method that was based on Levenberg–Marquard’s algorithm.⁴ The technique was used with care, to prevent the convergence at the local minima. The FAM and UPO cracking was observed to follow first-order kinetics.

(13) Wallenstein, D.; Alkemade, U. *Appl. Catal., A* **1996**, *137*, 37–54.

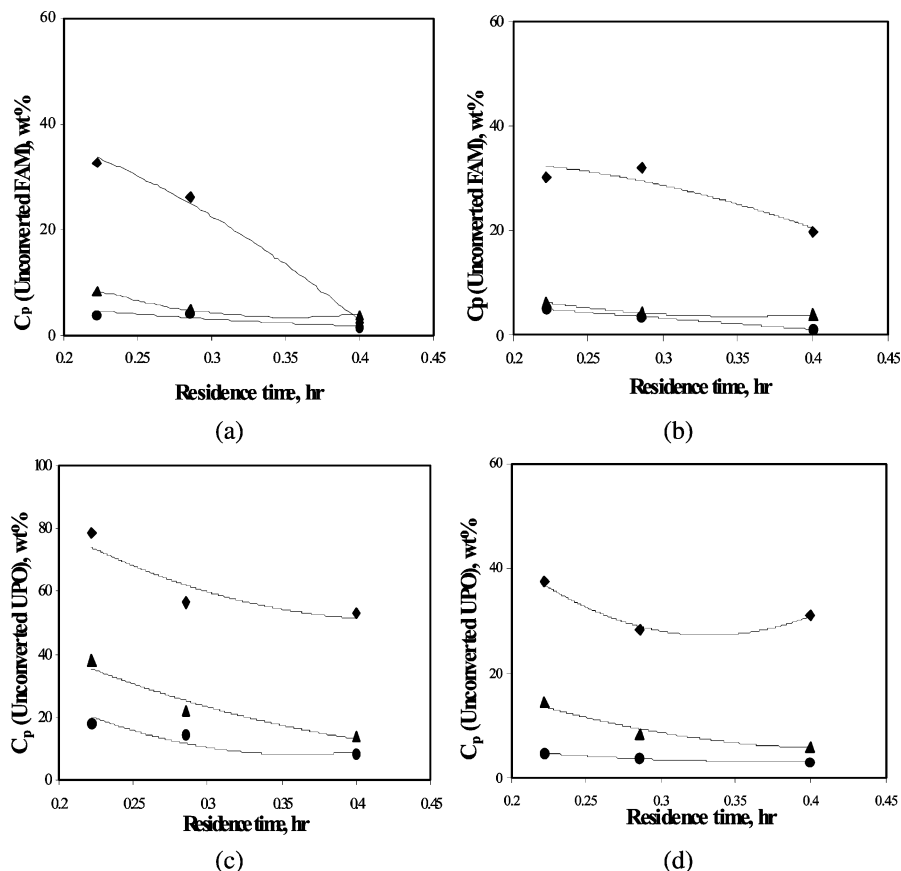


Figure 2. Polynomial fitting curves for the unconverted (a) FAM (HZSM-5), (b) FAM (CMZ20), (c) UPO (HZSM-5), and (d) UPO (CMZ40) at various temperatures ((♦) 673 K, (▲) 698 K, and (●) 723 K).

The four-lump model (see Figure 1b) was considered by separating the gaseous product and coke. The three-lump model provided the values of the kinetic parameters k_1 , k_2 , and k_3 , except for the rates of formation of gas and coke. The rate of gas formation is given by eq 10, and the rate of coke formation is given by eq 11.

$$\frac{dC_{\text{gas}}}{d\tau} = (k_{21}C_p + k_{31}C_{\text{OLP}} - k_4C_{\text{gas}})\varphi \quad (10)$$

$$\frac{dC_{\text{coke}}}{d\tau} = (k_{22}C_p + k_{32}C_{\text{OLP}} + k_4C_{\text{gas}})\varphi \quad (11)$$

where

$$k_2 = k_{21} + k_{22} \quad (12)$$

$$k_3 = k_{31} + k_{32} \quad (13)$$

The reaction constants k_{21} , k_{22} , k_{31} , k_{32} , and k_4 were estimated by solving eqs 10–13. The values of k_2 and k_3 obtained from the three-lump model were used to calculate k_{21} or k_{22} and k_{31} or k_{32} , using eqs 12 and 13,⁴ respectively. The estimated kinetic constants for the four-lump model are presented in Table 3 for FAM cracking and in Table 4 for UPO cracking.

To further split the OLP into more-detailed pseudo-components, based on their boiling range, a six-lump model was proposed (see Figure 1c). The OLP was separated into three lumps, which consisted of a gasoline fraction, a kerosene fraction, and a diesel fraction. The same procedure was repeated for the estimation of reaction constant, relative to the rate of reaction pre-

sented in eqs 14–18.⁴

$$\frac{dC_{\text{diesel}}}{d\tau} = (k_{11}C_p - k_5C_{\text{diesel}})\varphi \quad (14)$$

$$\frac{dC_{\text{kerosene}}}{d\tau} = (k_{12}C_p + k_{51}C_{\text{diesel}} - k_6C_{\text{kerosene}})\varphi \quad (15)$$

$$\frac{dC_{\text{gasoline}}}{d\tau} = (k_{13}C_p + k_{52}C_{\text{diesel}} + k_{61}C_{\text{kerosene}} - k_7C_{\text{gasoline}})\varphi \quad (16)$$

$$\frac{dC_{\text{gas}}}{d\tau} = (k_{21}C_p + k_{53}C_{\text{diesel}} + k_{62}C_{\text{kerosene}} + k_{71}C_{\text{gasoline}} - k_4C_{\text{gas}})\varphi \quad (17)$$

$$\frac{dC_{\text{coke}}}{d\tau} = (k_{22}C_p + k_{54}C_{\text{diesel}} + k_{63}C_{\text{kerosene}} + k_{72}C_{\text{gasoline}} + k_4C_{\text{gas}})\varphi \quad (18)$$

where

$$k_1 = k_{11} + k_{12} + k_{13} \quad (19)$$

$$k_5 = k_{51} + k_{52} + k_{53} + k_{54} \quad (20)$$

$$k_6 = k_{61} + k_{62} + k_{63} \quad (21)$$

$$k_7 = k_{71} + k_{72} \quad (22)$$

The estimated kinetic parameters for the six-lump model are presented in Table 3 for the cracking of FAM and Table 4 for the cracking of UPO at temperatures of 673, 698, and 723 K, respectively.

Table 3. Kinetic Constants Estimated from Three-, Four-, and Six-Lump Models for Fatty Acids Mixture (FAM) over HZSM-5 and CMZ20 at Different Operating Temperatures

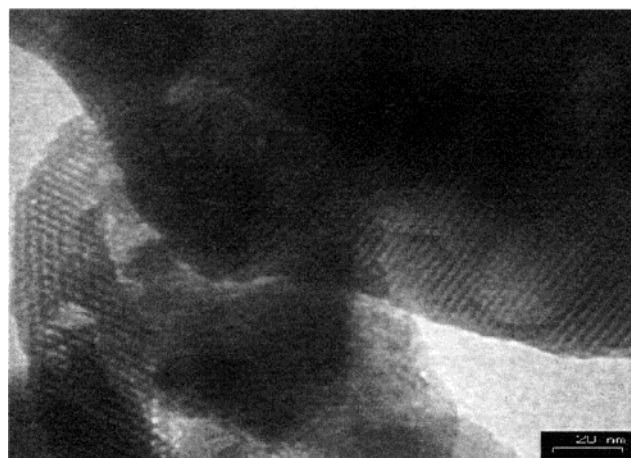
parameter	HZSM-5			CMZ20		
	673 K	698 K	723 K	673 K	698 K	723 K
Three-Lump Model						
k_1	5.3344	6.9924	7.6684	2.1970	4.6166	6.1724
k_2	0.3675	0.7631	1.1562	0.1007	0.2149	0.3008
k_3	0.0124	0.5879	0.7731	0.2987	0.4198	0.4327
Four-Lump Model						
k_{21}	0.3000	0.5385	0.8572	0.0983	0.2100	0.2830
k_{22}	0.0675	0.2246	0.2990	0.0024	0.0149	0.0178
k_{31}	0.0124	0.5879	0.7731	0.2987	0.4198	0.4327
k_{32}						
k_4						
Six-Lump Model						
k_{11}	0.2899	1.9171	2.0576	0.9212	1.0120	2.5184
k_{12}	2.2091	2.2300	2.2428	0.7703	1.6308	1.6540
k_{13}	2.8354	2.8453	3.3680	0.5055	1.9738	2.0000
k_{51}	1.8163	1.8170	1.9000			
k_{52}	0.0124	0.0831	0.2000	3.4521	3.4562	3.5000
k_{53}	0.0713	0.0800	0.1874	0.4205	0.6307	0.6328
k_{54}						
k_{61}				1.7984	1.8194	
k_{62}			1.9319	0.4143	1.3664	1.6394
k_{63}						
k_{71}	0.1120	0.4820	0.4925			1.4144
k_{72}						

Table 4. Kinetic Constants Estimated from Three-, Four-, and Six-Lump Models for Used Palm Oil over HZSM-5 and CMZ40 at Different Operating Temperatures

parameter	HZSM-5			CMZ40		
	673 K	698 K	723 K	673 K	698 K	723 K
Three-Lump Model						
k_1	1.4732	4.2290	6.3048	1.4709	5.1457	7.7156
k_2	1.1526	1.7196	1.7500	0.2012	0.2122	0.2494
k_3	0.0940	0.1067	0.1083	0.4829	0.5236	0.5457
Four-Lump Model						
k_{21}	0.7160	1.2200	1.2500	0.0895	0.0922	0.1000
k_{22}	0.4365	0.4996	0.5000	0.1117	0.1200	0.1494
k_{31}	0.0940	0.1067	0.1083	0.4829	0.5236	0.5457
k_{32}						
k_4	3.0395	0.4238	0.4227	2.0616	0.1237	0.1172
Six-Lump Model						
k_{11}	0.0792	0.6668	1.1798	0.4299	1.0500	3.1687
k_{12}	0.2415	2.3118	2.4011	0.0606	1.9850	2.4080
k_{13}	1.1526	1.2505	2.7239	1.3576	2.1107	2.1395
k_{51}	1.9000	1.9132	2.1022	1.0033	2.2920	3.1680
k_{52}	1.4852	1.4943	3.0312	2.0000	2.3700	2.4081
k_{53}	2.0206	2.1397	2.2407	0.8707	1.0904	1.2500
k_{54}						
k_{61}			1.4172			
k_{62}						
k_{63}						
k_{71}						
k_{72}						

5. Results and Discussion

The properties of the catalysts used in the present study are given in Table 5. As the the coating layer of MCM-41 over ZSM-5 was increased, the BET surface area was increased from 367 m²/g to 614 m²/g and the acidity value decreased from 0.21 mmol H⁺/g cat to 0.09 mmol H⁺/g cat. The pure mesoporous silica did not contribute any acidity to the catalyst, and, therefore,

**Figure 3.** Transmission electron microscopy (TEM) image of composite CMZ40.

the overall acidity value decreased. Figure 3 shows the TEM image of the composite CMZ40. The composite catalyst has a uniform hexagonal unidimensional mesopore structure, which confirmed the presence of MCM-41. As the physicochemical properties of the catalyst—especially, the accessibility of the feedstock in the pore structure—changed, their influences in the kinetic model were studied and compared.

Figure 4 shows the conversion of FAM and UPO against WHSV. It can be observed that the conversion of FAM and UPO linearly decreased with WHSV for all operating temperatures. The lower reaction temperature and higher slope of the graph indicated that WHSV gave a more significant effect at low temperature, in terms of conversion. The composite catalyst with lower acidity was determined to be moderately more active than HZSM-5. The higher activity was due to the less-pronounced effect of intraparticle diffusion in the composite catalyst for UPO cracking, showing the role of mesoporous MCM-41 in the composite. Using a different feedstock, HZSM-5 gave higher conversion in FAM cracking, compared to UPO cracking. This was caused by the higher percentage of saturated fatty acids in UPO, which gave a lower rate of cracking, as compared to FAM with a higher content of more-reactive unsaturated fatty acids.¹⁴ The predicted values showed larger deviation at a reaction temperature of 673 K than at higher reaction temperatures. This may due to a different route of the cracking mechanism, as compared to the reaction mechanism at higher reaction temperatures.

The reaction rate constants for FAM and UPO cracking presented in Tables 3 and 4 show that the reaction rate constants increased significantly with the reaction temperature. By comparing the catalysts used for the cracking of FAM, the composite catalyst gave relatively lower rate-constant values, whereas the opposite trend was observed for the cracking of UPO. The coating of a silica layer on ZSM-5 reduced the acidity of the catalyst. Hence, the cracking rates were decreased, resulting in

Table 5. Physicochemical Properties of the Catalysts

catalyst	BET surface area (m ² /g)	pore volume at $P/P_0 = 0.5$ (cm ³ /g)	average pore size (nm)	acidity (mmol H ⁺ /g cat)
HZSM-5	367	0.21		0.21
CMZ20	400	0.24	2.37	0.13
CMZ40	614	0.44	2.84	0.09

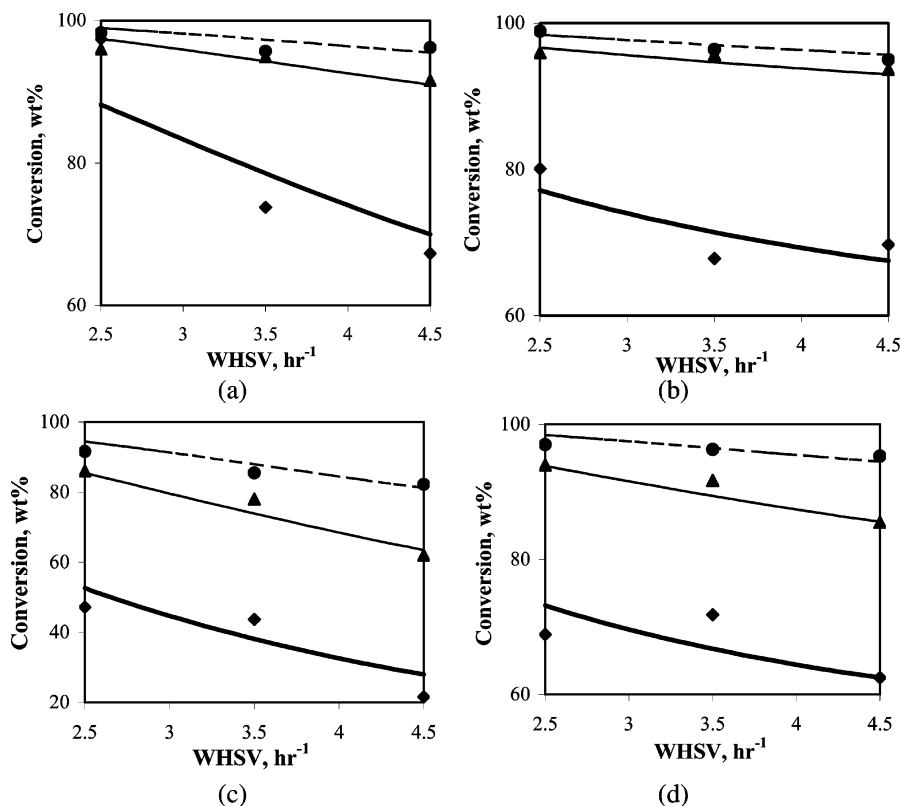


Figure 4. Conversion of (a) FAM (HZSM-5), (b) FAM (CMZ20), (c) UPO (HZSM-5), and (d) UPO (CMZ40) at various temperatures ((♦) 673 K, (▲) 698 K, and (●) 723 K), compared with the values obtained from the models (lines).

Table 6. Comparison of Activation Energies with Gas Oil Cracking from the Literature

reaction	Activation Energy, E (kJ/mol)				
	FAM (HZSM-5) ^a	FAM (CMZ20) ^a	UPO (HZSM-5) ^a	UPO (CMZ40) ^a	gas oil ^b
FAM/UPO → organic liquid product (OLP)	30	84	118	116	42–151
FAM/UPO → gas + coke	93	89	34	17	38–75
FAM/UPO → gas	85	89	46	9	50–100
FAM/UPO → coke	121	169	11	23	29–67
FAM/UPO → gasoline	14	6	69	37	42–151
FAM/UPO → kerosene	1	63	188	301	
FAM/UPO → diesel	160	115	220	161	
gasoline → gas	121				54–126
deactivation	5	7	8	41	75

^a Fatty acids mixture (FAM) or used palm oil (UPO) cracked over the catalyst listed in parentheses. ^b Gas oil cracked over different FCC catalysts, from literature.⁶

the lower value of reaction rate constants in the cracking of FAM. In the cracking of UPO, saturated fatty acids initiated the cracking by producing olefin from the thermal cracking. With the increased surface area of the composite catalyst, the cracking rate increased, resulting in higher rate-constant values.

A major objective of the present study was to determine the role of the catalysts in the gasoline fraction yield from the FAM/UPO cracking. The gasoline fractions decreased as the residence time at higher reaction temperature increased for the cracking of FAM over HZSM-5. It was observed that the reaction rate constant for the decomposition of the gasoline fraction was negligible, with the exception of the formation of gas from gasoline decomposition when a composite catalyst was used, except at 723 K. This result suggested that the overcracking reaction was hindered by the moderate acidity of the composite catalyst. Nevertheless, at higher reaction temperature, hydrogen transfer reaction was

depressed and therefore gasoline yield was reduced.¹⁵ The same observation also occurred in the UPO cracking; however, gasoline cracking remained stable, because the reaction rate constants k_{71} and k_{72} for gas or coke formation from the gasoline fraction were negligible. The rate constant values showed that the kerosene fractions did not undergo secondary cracking reactions, when comparing the k values for the decomposition of the diesel fraction, indicating that secondary cracking reactions occurred. However, CMZ20 in the presence of mesophase encouraged decomposition of the kerosene fraction toward gas formation through a secondary cracking reaction.

The activation energy required for the cracking was calculated from the Arrhenius plots of the respective rate constants. The activation energy was determined to be dependent on the type of feedstock and catalyst used. The activation energy values were comparable with those of the cracking of gas oil,⁶ except for the

(14) Rase, H. F. *Handbook of Commercial Catalysts*; CRC Press: Boca Raton, FL, 2000.

(15) Gianetto, A.; Farag, H. I.; Blasetti, A. P.; de Lasa, H. I. *Ind. Eng. Chem. Res.* **1994**, *33*, 3053–3062.

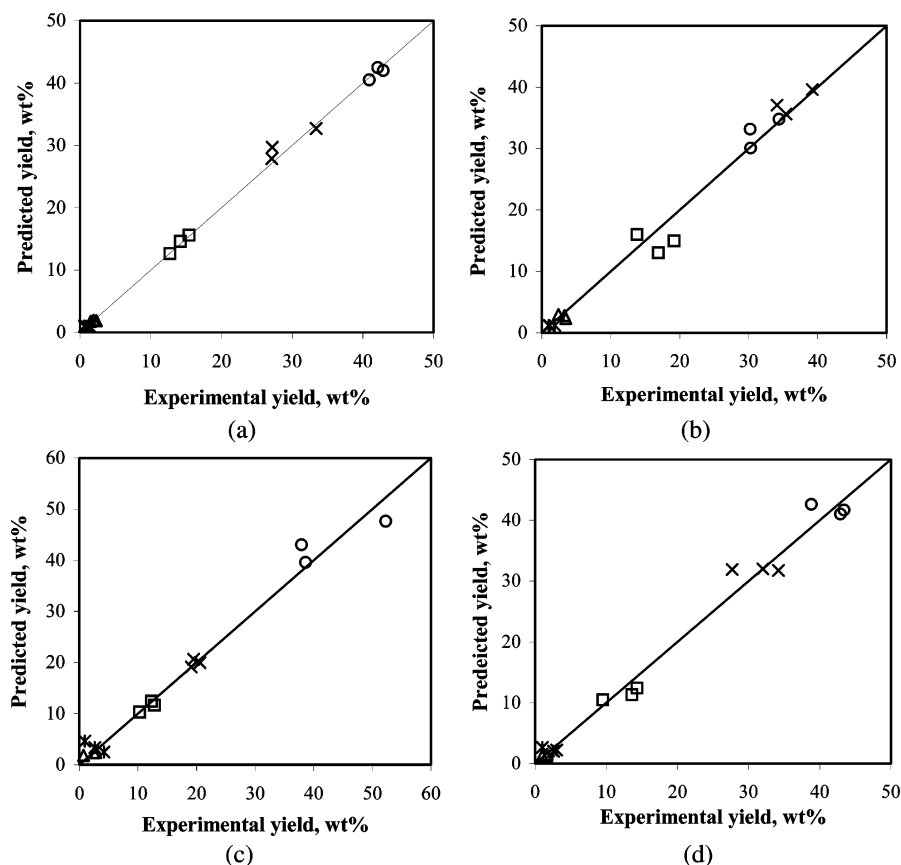


Figure 5. Predicted versus experimental yields of (○) gasoline, (□) kerosene, (△) diesel, (×) gas, and (▲) coke for (a) FAM (HZSM-5), (b) FAM (CMZ20), (c) UPO (HZSM-5), and (d) UPO (CMZ40) at 723 K.

reaction of FAM to coke and gasoline and the UPO reaction to gas over CMZ40. Table 6 presents a comparison of the activation energies obtained in the present study with the reported values of activation energies for the gas oil cracking. The lower activation energy was due to the presence of triglycerides and oxygen, which are very active to form carbenium ions on the catalyst, which enable the cracking that occurred at lower activation energy. The deactivation energies were also lower than that of gas oil cracking.

Equations 6 and 14–18 were integrated simultaneously, using the Runge–Kutta–Fehlberg (RKF) algorithm in the residence time range of 0.25–0.4 h to predict the conversion and yield of products. The predicted product yields obtained from the six-lump model versus the experimental data are presented in Figure 5. The model could be used to predict values in the range of the variables studied. The adequacy of the kinetic model was confirmed by the small deviation (<10% error) that was observed between the predicted product yield and the experimental values.

6. Conclusions

The sequential estimation of the kinetic parameters proposed by Ancheyta-Juarez et al.⁴ from three-, four-, and six-lump models reduced the number of simultaneously estimated parameters in the cracking of fatty acids mixture (FAM) and used palm oil (UPO). The models developed gave useful information, in regard to the role of composites in the catalytic cracking process and activation energy. The composition of feedstock affected the conversion as well as the product distribu-

tion during the cracking process. The reaction rate parameters were dependent on the type of feedstock. Using a composite catalyst, the diffusional constraint was reduced, resulting in higher conversion during the cracking reaction.

Acknowledgment. The authors would like to acknowledge the research grant provided by the Ministry of Science, Technology and Environment, Malaysia, under a Long Term IRPA Grant (Project No. 02-02-05-2184 EA005), which has resulted in this article.

Nomenclature

C_P = unconverted FAM/UPO weight fraction (wt %)

C_{product} = product weight fraction (wt %)

E = activation energy (kJ/mol)

FAM = fatty acids mixture

k = reaction rate constant (h^{-1})

k_d = deactivation rate constant (h^{-1})

n = reaction order

n_d = deactivation order

t = time on stream (h)

UPO = used palm oil

WHSV = weight hourly space velocity ($\text{kg}_{\text{feed}} \text{kg}_{\text{catalyst}}^{-1} \text{h}^{-1}$)

Greek Symbols

φ = deactivation function

τ = residence time (h)

EF049948V